Photochemical Modification and Patterning of Polymer Surfaces by Surface Adsorption of Photoactive Block Copolymers

F. Pan, P. Wang, K. Lee, A. Wu, N. J. Turro, and J. T. Koberstein*

Departments of Chemistry and Chemical Engineering, Columbia University, 500 West 120th Street, MC4721, New York, New York 10027

Received September 9, 2004. In Final Form: February 2, 2005

We report a simple photolithographic approach for the creation and micropatterning of chemical functionality on polymer surfaces by use of surface-active block copolymers that contain protected photoactive functional groups. The block copolymers self-assemble at the substrate−air interface to generate a surface that is initially hydrophobic with low surface tension but that can be rendered hydrophilic and functional by photodeprotection with UV radiation. The block copolymer employed, poly(styrene-*b*-*tert* butyl acrylate), segregates preferentially to the surface of a polystyrene substrate because of the low surface tension of the polyacrylate blocks. The strong adsorption of block copolymers causes a bilayer structure to form presenting a photoactive polyacrylate layer at the surface. In the example described, the *tert*-butyl ester groups on the polyacrylate blocks are deprotected by exposure to UV radiation in the presence of added photoacid generators to form surface carboxylic acid groups. Surface micropatterns of carboxylic acid groups are generated by UV exposure through a contact mask. The success of surface chemical modification and pattern formation is demonstrated by X-ray photoelectron spectroscopy and contact angle measurements along with imaging by optical and fluorescence microscopy methods. The resultant chemically patterned surfaces are then used to template patterns of various biomolecules by means of selective adsorption, covalent bonding and molecular recognition mechanisms. The surface modification/patterning concept can be applied to virtually any polymeric substrate because protected functional groups have intrinsically low surface tensions, rendering properly designed block copolymers surface active in almost all polymeric substrates.

Introduction

The modification of polymer surface properties is a subject of great general interest because most polymers have an intrinsically low surface tension, requiring that the chemical nature of their surfaces be altered to achieve desirable adhesion, wettability, and biocompatibility. In many applications, methods such as plasma or chemical treatments,[1] designed to increase surface tension by surface oxidation, are sufficient to provide the desired surface modifications. Many of these methods, however, are brute force in nature and do not provide for accurate control of variables such as the chemical nature or depth of the surface modification. The surfaces they produce are thermodynamically unstable and subject to reorganization effects. More recently, attention has focused on surface modification methods that can be used to precisely fabricate polymer surfaces with controlled surface density of particular functional groups. Functional groups may be initiators for subsequent surface initiated polymerization or grafting, intermediates for further surface derivatization reactions, or reactive sites for bioconjugation with peptides and proteins. High-energy (i.e., high surface tension) functional groups, however, are naturally repelled from polymer surfaces leading to surface compositions that can be much lower than that of the bulk material.[2−5] Moreover, functional polymer surfaces are subject to surface reorganization phenomena when moved from one environment to another.[6,7] These factors render precise fabrication of functional polymer surfaces a difficult task. Recent publications by our own and other groups have led to the establishment of several fundamental principles that allow for the molecular design of functional polymer surfaces.[8]

It is also desirable to control the spatial distribution or pattern of surface chemical species created during polymer surface modification. Current applications in microelectronics, information storage, optics, microarray/diagnostic sensors, and microfluidics call for polymer surfaces that are patterned on micrometer or submicrometer size scales with different chemical functionalities (or controlled properties such as hydrophobicity or wettability). Micropatterned surfaces serve as important templates for selective deposition of metal oxides,[9,10] polymers,[11−13] organic and inorganic colloidal particles,[14−17] nanoparticles,[18−22] and

* To whom correspondence should be addressed: phone, (212) 854-3120; fax, (212) 854-3054; e-mail, jk1191@columbia.edu.

(1) For general references see: (a) Wu, S. In *Polymer Interface and Adhesion*; Marcel Dekker: New York, 1982. (b) Garbassi, F.; Morra, M.; Occhiello, E. In *Polymer Surfaces*: *From Physics to Technology*; Wiley: New York, 1999.

(2) Jalbert, C. A.; Balaji, R.; Bhatia, Q.; Koberstein, J. T.; Salvati, L., Jr.; Yilgor, I. *Macromolecules* **1994**, *27*, 2409.

(3) (a) Theodorou, D. N. *Macromolecules* **1988**, *21*, 1411. (b) Theodorou, D. N. *Macromolecules* **1988**, *21*, 1422.

(4) Jalbert, C. A.; Koberstein, J. T.; Hariharan, A.; Kumar, S. K. *Macromolecules* **1997**, *30*, 4481.

(5) O'Rourke-Muisener, P. A. V.; Kumar, S. K.; Koberstein, J. T. *Macromolecules* **2003**, *36*, 771.

(6) Holly, F. J.; Refojo, M. F. In *Hydrogels for Medical and Related Applications*; Andrade, Ed.; ACS Symposium Series 31; American Chemical Society: Washington, DC, 1976.

(7) Koberstein, J. T. *MRS Bull.* **1996**, *21* (1), 19.

(8) Koberstein, J. T. *J. Polym. Sci., Polm. Phys. Ed.* **2004**, *42*, 2942.

(9) Kumar, A.; Whitesides, G. M. *Appl. Phys. Lett*. **1993**, *63*, 2002.

(10) Jeon, N. L.; Clem, P. G.; Nuzzo, R. G.; Payne, D. A. *J. Mater. Res*. **1995**, *10*, 2996.

(11) Prucker, O.; Schimmel, M.; Tovar, G.; Knoll, W.; Ruhe, J. *Adv. Mater*. **1998**, *10*, 1073.

(12) Maeng, I. S.; Park, J. W. *Langmuir* **2003**, *19*, 9973.

(13) Lee, S. K.; Jung, B.-J.; Ahn, T.; Song, A.; Shim, H.-K. *Macromolecules* **2003**, *36*, 9252.

(14) Kruger, C.; Jonas, U. J. *Colloid Interface Sci.* **2002**, *252*, 331.

(15) Sun, Y. J.; Walker, G. C. *J. Phys. Chem. B* **2002**, *106*, 2217.

(16) Fudouzi, H.; Kobayashi, M.; Shinya, N. *Langmuir* **2002**, *18*, 7648.

(17) Fan, F. Q.; Stebe, K. J. *Langmuir* **2004**, *20*, 3062.

10.1021/la0477439 CCC: $30.25
Published on Web 03/10/2005

biomolecules[23] such as DNA, proteins, peptides, and cells.

A number of techniques have been successfully developed for micropatterning organic substances onto solid substrates such as metals, glass, and silicon. These micropatterning approaches include photochemical methods such as photolithography,[24,25] laser ablation,[26] ion and e-beam writing,[27,28,29] photoimmobilization,[30] and surface-initiated polymerization;[11,31] mechanical means including inkjet printing,[32] microcontact printing,[33] and micromachining;[34] and electrochemical methods.[35] Many of these techniques are based upon coating the substrates with self-assembled monolayers (SAMs) of organosilanes (for glass and silicon substrates) and alkanethiols (for gold substrates) because they form uniform films of the appropriate thickness and can be designed to present a functional surface.

Far fewer examples exist for surface micropatterning on polymeric substrates. Biological ligands have been patterned directly on polymeric substrates using microcontact printing;[36−41] however the technique usually requires prior chemical activation of the polymer surface using surface derivatization reactions that are difficult to control. Protein microarrays have also been prepared by noncontact microdispensing of protein solutions;[42] however the technique again requires a first step, chemical activation of the polymer surface as well as a second step involving covalent bioconjugation. It was recently demonstrated that polymer surfaces could be patterned with cells without the requirement of a chemical activation step. Microcontact printing was used to form a pattern of amphiphilic comb polymers on a polystyrene surface[43] that templated the adsorption of fibronectin, an extracellular matrix protein that directs cell adhesion. Exposure to endothelial cells produced a micropattern of cells that corresponded to the original pattern of the comb polymer.

Polymer surfaces have also been patterned by chemical methods including photolithography[44] and surface photografting/polymerization techniques.[45−50] Photografting methods are based upon incorporation of photoactive monomers into the polymeric substrate. The usual procedure involves forming a layer of a second polymer or biomacromolecules on top of the photoactive substrate and photografting in a desired pattern by exposure to UV radiation through a mask.

In this paper, we illustrate a new approach to chemically modify and pattern polymer surfaces that is applicable for almost all polymeric substrates. The method employs photoactive diblock copolymers that segregate preferentially at the surface of most polymeric substrates. The copolymer comprises one photoactive block that has a low surface tension and that can be chemically transformed by exposure to UV radiation and a second so-called "anchor" block that consists of the same polymer as the polymeric substrate. Once adsorbed at the surface of the polymeric substrate, the copolymer self-assembles to form a bilayer structure wherein the photoactive copolymer sequence forms a layer at the surface and the anchor block forms a second layer interpenetrated with the substrate polymer. The latter characteristic ensures that the copolymer layer is well anchored into the polymeric substrate

The surface layer comprising the photoactive copolymer sequence is chemically modified, for example, transformed from hydrophobic to hydrophilic character, by applying chemical amplification photolithography[51] strategies used extensively in current photoresist technology. The key to chemically amplified technology is the use of catalysts called photoacid generators (PAGs) that produce a strong acid upon exposure to deep UV (DUV) radiation (248 and 193 nm). In the example described herein, a PAG is used to generate a small amount of strong acid that catalyzes the hydrolysis or deprotection of *tert*-butyl pendant groups on poly(styrene-*b*-*tert*-butyl acrylate) (P(S-*b*-tBA)) block copolymers adsorbed at the surface of a PS substrate. Deprotection in this manner creates surface-bound carboxylic acid groups. The acrylates function well in this application because they have well-defined and reliable DUV photochemistry,[31,52] they have the low surface tensions required (24−28 mN/m) to drive surface segregation and self-assembly, and they are biocompatible photoresists[53,54] known to be tolerated by biomolecules that might be immobilized onto such a surface.

Patterns of surface functional groups are created by simply exposing the photoactive block polymer surface

(18) Lee, K. J.; Pan, F.; Carroll, G. T.; Turro, N. J.; Koberstein, J. T. *Langmuir* **2004**, *20*, 1812.
(19) Phely-Bobin, T. S.; Muisener, R. J.; Koberstein, J. T.; Papadimitrakopoulos, F. *Synth. Met.* **2001**, *116*, 439.
(20) Phely-Bobin, T. S.; Muisener, R. J.; Koberstein, J. T.; Papadimitrakopoulos, F. *Adv. Mater* **2000**, *12*, 1257.
(21) Hua, F.; Cui, T. H.; Lvov, Y. *Langmuir* **2002**, *18*, 6712.
(22) Ryan, D.; Nagle, L.; Fitzmaurice, D. *Nano Lett*. **2004**, *4*, 5573.
(23) For reviews, see for example: (a) Blawas, A. S. *Biomaterials* **1998**, *19*, 595. (b) Kane, R. S.; Takayama, S.; Ostuni, E.; Ingber, D. E.; Whitesides, G. M. *Biomaterials* **1999**, *20*, 2362. (c) Suh, K. Y.; Seong, J.; Khademhosseini, A.; Laibinis, P. E.; Langer, R. *Biomaterials* **2004**, *25*, 557.
(24) Xia, Y.; Whitesides, G. M. *Annu. Rev. Mater. Sci*. **1998**, *28*, 153.
(25) Pritchard, D. J.; Morgan, H.; Cooper, J. M. *Angew. Chem., Int. Ed. Engl.* **1995**, *34*, 91.
(26) Vaida, R. Tender, L. M.; Bradley, G.; O'Brien, M. J.; Cone, M.; Lopez, G. P. *Biotechnol. Prog.* **1998**, *14*, 371.
(27) Matsui, S.; Kojima, Y.; Ochiai, Y. *Appl. Phys. Lett*. **1988**, *53*, 868.
(28) Perkins, F. K.; Dobisz, E. A.; Brandow, S. L.; Calvert, J. M.; Kosakowski, J. E.; Marrian, C. R. K. *Appl. Phys. Lett*. **1996**, *68*, 550.
(29) Ada, E. T.; Hanley, L.; Etchin, S.; Melngailis, J.; Dressick, W. J.; Chen, M. S.; Calvert, J. M. *J. Vac. Sci. Technol., B* **1995**, *13*, 2189.
(30) Delamarche, E.; Sudarababu, G.; Biebuyck, H.; Michel, B.; Gerber, C.; Sigirst, H.; Wolf, H.; Ringsdorf, H. Xanthopoulos, N.; Mathieu, H. J. *Langmuir* **1996**, *12*, 1997.
(31) Husemann, Mm.; Morrison, M.; Beniot, D.; Frommer, J.; Mate, C. M.; Hinsburg, W. D.; Hedrick, J. L.; Hawker, C. J. *J. Am. Chem. Soc.* **2000**, *122*, 1844.
(32) Calvert, P. *Chem. Mater*. **2001**, *13*, 3299.
(33) Xia, Y.; Whitesides, G. M. *Angew. Chem., Int. Ed*. **1998**, *37*, 550.
(34) Abbot, N. L.; Folkers, J. P. Whitesides, G. M. *Science* **1992**, *257*, 1380.
(35) Tender, L. M.; Worley, R. L.; Fan, H. Y.; Lopez, G. P. *Langmuir* **1996**, *12*, 5515.
(36) Patel, N.; Padera, R.; Sanders, G. H. W.; Cannizaro, S. M.; Davies, M. C.; Langer, R.; Roberts, C. J.; Tendler, S. J. B.; Williams, P. M.; Shakesheff, K. M. *FASEB J.* **1998**, *12*, 1447.
(37) Yang, A.; Chilkotli, A. *Adv. Mater*. **2000**, *12*, 413.
(38) Yang, Z.; Belu, A. M.; Liebmann-Vinson, A.; Sugg, H.; Chilkoti, A. *Langmuir* **2000**, *16*, 7482.
(39) Hyun, J.; Zhu, Y.; Liebmann-Vinson, A.; Beebe, T. P., Jr.; Chilkoti, A. *Langmuir* **2001**, *17*, 6358.
(40) Hyun, J.; Ma, H.; Banerfee, P.; Cole, J.; Gonsalves, K.; Chilkoti, A. *Langmuir* **2002**, *18*, 2975.
(41) Lee, K.-B.; Kim, D. J.; Lee, Z.-W.; Woo, S. I.; Choi, I. S. *Langmuir* **2004**, *20*, 2531.
(42) Charles, P. T.; Taitt, C. R.; Goldman, E. R.; Rangasammy, J. G.; Stenger, D. A. *Langmuir* **2004**, *20*, 270.
(43) Hyun, J.; Ma, H.; Zhang, Z.; Beebe, T. P., Jr.; Chilkoti, A. *Adv. Mater*. **2003**, *15*, 576.
(44) He, W.; Halberstadt, C. R.; Gonsalves, K. E. *Biomaterials* **2004**, *25*, 2055.
(45) Nakayama, T.; Matsuda, T. *Macromolecules* **1996**, *29*, 8622.
(46) Nakayama, T.; Matsuda, T. *Langmuir* **1999**, *15*, 5560.
(47) Ward, J. H.; Bashir, R.; Peppas, N. A. J. *Biomed. Mater. Res.* **2001**, *56*, 351.
(48) Lahann, J.; Choi, I. S.; Lee, J.; Jensen, K. F.; Langer, R. *Angew. Chem., Int. Ed*. **2001**, *40*, 3166.
(49) Lahann, J.; Balcells, M.; Rodon, T.; Lee, J.; Choi, I. S.; Jensen, K. F., Langer, R. *Langmuir* **2002**, *18*, 3632.
(50) Luo, N.; Metters, A. T.; Hutchinson, J. B.; Bowman, C. N.; Anseth, K. S. *Macromolecules* **2003**, *36*, 6739.
(51) Ito, H.; Wilson, C. G.; Frechet, J. M.; Farral, M. J.; Eichler, E. *Macromolecules* **1983**, *16*, 510.
(52) Ito, H. *Jpn. J. Appl. Phys.* **1992**, *31*, 4273.

layer to DUV through a contact mask. The result is a spatial pattern of alternating hydrophobic *tert*-butyl groups and hydrophilic carboxylic acid groups at the surface. We demonstrate that surface-active block copolymers with protective functional groups, such as surface-active block copolymers with functional end groups described previously by our group,[55] are a precise and effective means to functionalize the surfaces of polymeric substrates and to create patterns of surface functional groups on polymeric substrates. In that sense, the general method of using surface-active block copolymers with protected functional groups to modify polymeric substrates is analogous to the use of self-assembled monolayers to functionalize and pattern the surfaces of glass, gold, and other inorganic solid substrates.

Experimental Section

Materials. PS (250 kDa) was purchased from Acros Organics Inc. The P(S-*b*-tBA) block copolymer has reported molecular weights of 200 kDa for each block. The block copolymer was purchased from Polymer Source Inc. Coupling agents 1-ethyl-3-(3-dimethylaminopropyl)carbodiimide hydrochloride (EDC) and *N*-hydroxyl succinimide (NHS) were purchased from Aldrich. Triphenylsulfonium triflate, the photoacid generator (PAG), was a gift from IBM. Solvents including toluene (99.5% purity) and propylene glycol methyl ether acetate (PGMEA, 99% purity) were purchased from Aldrich. Ethanol (absolute) was purchased from Pharmcoproducts. Most of the organic dyes and fluorescent-tagged biomolecules were purchased from Molecular Probes Inc., including 4,4-difluoro-1,3,5,7-tetramethyl-4-bora-3a,4a-diaza-s-indacene-8-propionic acid succinimidyl ester (BODIPY 493/503, SE, referred to as Bodipy-ester in this paper), 4,4-difluoro-5,7-dimethyl-4-bora-3a,4a-diaza-s-indacene-3-propionyl ethylenediamine hydrochloride (BODIPY FL EDA, termed as Bodipy-NH_2 in this paper), *N*-(2-aminoethyl)biotinamide hydrobromide (biotin ethylenediamine, referred to as Biotin-NH_2 in this paper), and Alexa488 tagged Streptavidin (Streptavidin−Alexa488). Fluorescein-5 isothiocyanate tagged bovine serum albumin (BSA−FITC) was a generous gift from Professor Robert Prud'homme from Princeton University.

Sessile drop water contact angle measurements were carried out at room temperature with a model 100-00 contact angle goniometer (Rame-Hart, Inc.). The contact angles were recorded immediately after dispensing 1−10 μL water droplets with a pipet onto the surface. The reported values were average values of measurements for more than three different samples at more than three different locations for each sample.

X-ray photoelectron spectroscopy spectra were recorded with a PHI 5500 spectrometer equipped with a hemispherical electron energy analyzer, a multichannel detector, and a Al Kα monochromator X-ray source run at 15 kV and 23.3 mA. The test chamber pressure was maintained below 2×10^{-9} Torr during spectral acquisition. A low-energy electron flood gun was used as required to neutralize surface charging. The X-ray photoelectron spectroscopy (XPS) binding energy (BE) was internally referenced to the aliphatic C 1s peak at 284.6 eV. Survey spectra were acquired using an analyzer pass energy of 93.9 eV and a BE resolution of 0.8 eV, while high-resolution spectra were acquired with a pass energy of 23.5 eV and a BE resolution of 0.05 eV. The takeoff angle is defined as the angle between the surface and the photoelectron detector. Angle-dependent XPS (ADXPS) was performed by rotating the sample holder to the desired photoelectron takeoff angle. Spectra were deconvoluted using PHI data processing software that fits a series of Gaussian−Lorentzian functions to each chemically shifted photoelectron peak after subtracting an appropriate background. Atomic concentrations were calculated by normalizing peak areas with the elemental sensitivity factor data provided in the PHI database.

Fluorescence imaging was carried out using an Olympus IX70 laser scanning confocal microscope equipped with an argon ion laser as the excitation source. Fluorescence was excited at 488 nm, and emission was collected above 510 nm after passing through a 510 nm long pass filter. Fluorescence intensity was monitored as a function of X−Y position as the sample was focused above the laser beam through 20× or 10× objectives. Fluorescence images (512 × 512 pixels) were typically acquired at a PMT voltage of 900 V and a scan speed of 16 s per scan. Light micrographs were recorded with a Nikon OPTIPHOT metallurgical dark field microscope equipped with a Kodak MDS digital camera in the reflection mode. Images were typically acquired using 20× or 5× objectives.

The thickness of polymer thin films was measured with a Beaglehole spectroscopic and imaging ellipsometer (Beaglehole Instruments, Wellington, New Zealand) under variable angle mode from 65° to 75° with a fixed wavelength of 632.8 nm. The final thickness data were averaged over multiple measurements (greater than five) taken at different locations on different samples. The measured ellipsometry data were analyzed using Film Wizard software. During the optimization to experiment, the thickness of the film was the only parameter adjusted while all other variables were kept constant. Conventional values for the optical constants of the substrate, silicon wafer, were used: $n \sim 3.59-3.60$, $k \sim 0.015-0.025$. The optical constants of the polymer thin films were assumed to be identical to their bulk values, for example, $n(\mathrm{PS}) = 1.59$ and $k(\mathrm{PS}) = 0$. Optimization of the experiment was regarded as successful only when the root-mean-squared error was less than 0.3 and the measured n and k of the polymer films as a function of the angle were in visual agreement with the simulation results.

Glass substrates (coverslips or slides) were cleaned by soaking in NaOH/H_2O/ethanol mixture (1:1:8 w/w) for 10 min. Si substrates were cleaned by exposure to UV and ozone for 15 min and then washing extensively with deionized (DI) water and acetone. For patterning experiments, a 40 nm layer of pure PS (MW = 250K) was spin coated from a 0.77% w/w solution of PS in toluene onto cleaned substrates. A 20 nm layer of block copolymer was subsequently spin coated from a solution of 0.46% w/w polymer in toluene on top of the PS substrate. To study the annealing effect on the self-assembly process of the diblock copolymer and to control the acrylate block layer thickness, films were prepared by spin coating at 2400 rpm from block copolymer solutions in toluene with concentrations ranging from 0.1 to 0.6 wt %. The resultant films were annealed at 110 °C in a vacuum for over 12 h.

A layer of PAG was spin coated (1000 rpm, 1 min) on top of the copolymer/PS/glass substrate from a solution of PAG in ethanol (1.5% w/w). The resultant PAG/copolymer/PS/glass samples were placed under a hand-held UV lamp and exposed to DUV (254 nm wavelength, 760 μW/cm^2) for 5 min (with a photomask in contact with the sample on the top in the case of patterning). If necessary, the UV-exposed sample was postbaked at 100 °C for 30 s to a few minutes to facilitate the diffusion of photogenerated acids and thereby increase the degree of *tert*-butyl ester deprotection. Excess PAG was washed away by ethanol after which the sample was dried with nitrogen.

Samples with patterned surfaces were subsequently treated in several ways to examine whether they supported selective deposition of biomolecules. Some patterned surfaces were immersed overnight in 10 μM solutions of Bodipy-NH_2 or Bodipy-ester in ethanol and then N_2 dried after removal from the solution. Immobilization of BSA−FITC was achieved by immersing surface-patterned substrates into an ethanol solution of BSA−FITC (10 μM) overnight, followed by drying in nitrogen. Biotin/Strepavidin−Alex488 was patterned by a covalent amide linkage in a multistep derivatization procedure. First the carboxylic acid sites of the surface-patterned polymer substrate were activated by immersion into a DI water solution containing EDC (0.1 M) and NHS (0.2 M) for 1 h. Then biotin-NH2 ligands were covalently bound to the activated surface COOH sites through an amide linkage by immersing the COOH-activated surface-patterned polymeric substrate into an ethanol solution of Biotin-NH_2 (10 mM) for 1 h. The samples were then washed with DI water and ethanol. Finally, the molecular recognition step between surface-bound Biotin and Streptavidin−Alexa488 was completed by

(53) Douvas, A.; Argitis, P.; Diakoumakos, C. D.; Misiakos, K.; Dimotikali, D.; Kakabakos, S. E. *J. Vac. Sci. Technol., B* **2001**, *19*, 2820.
(54) Douvas, A.; Argitis, P.; Misiakos, K.; Dimotikali, D.; Petrou, P.; Kakabakos, S. E. *Biosens. Bioelectron.* **2002**, *17*, 269.
(55) Koberstein, J. T.; Duch, D. E.; Hu, W.; Lenk, T. J.; Bhatia, R.; Brown, H. R.; Lingelser, J. P.; Gallot, Y. *J. Adhes.* **1998**, *66*, 229.

immersing Biotin-bound samples for 4−12 h in a solution of 10 μM Streptavidin−Alexa488 in HEPES buffer (pH = 7.4) which also contained 0.1% (w/w) BSA and 0.02% (v/v) Tween 20 detergent. The samples were then dried in nitrogen and washed with HEPES buffer.

Results and Discussion

The first step in our approach for polymer surface modification is the molecular design of a polymer architecture that can deliver a photoactive polymer to the surface of a polymeric substrate. The goal here is to provide modification of the surface without changing the bulk material properties. In the example described herein, we choose a molecular design which uses a self-assembly process to create the modified polymer surface. The basis of the molecular design is the fact that block copolymers with one low surface tension block are known to spontaneously self-assemble at the surface of a homopolymer matrix of higher surface tension.[56,57] We then take advantage of the fact that most schemes for protection of reactive functional groups employ protecting groups that have intrinsically low surface tensions. Common protecting groups such as trimethylsilane and *tert*-butoxy, for example, impart low surface tension when used to protect a functional polymer because they contain three low-energy methyl groups. In the current work, we employ poly(*tert*-butyl acrylate), with a surface tension of only 30.4 mN/m, as the low surface tension block of the surface-active block copolymer; however, many other "protected" functional polymers could also be used in this application.

The model system chosen for study is a surface-active P(S-*b*-tBA) diblock copolymer for the modification of a polystyrene substrate. These block copolymers self-assemble readily at the surface of a higher surface tension polystyrene substrate (surface tension of 40 mN/m) and contain protected carboxylic acid functionality that can be regenerated by photolysis of the ester group. Symmetric diblock copolymers were chosen to favor self-organization into a lamellar bilayer structure that presents a polyacrylate layer at the surface.

The block copolymers may be delivered to the surface by a number of different strategies. The block copolymer may be mixed within the matrix polymer and allowed to spontaneously assemble from the bulk phase; however, the rate of diffusion of block copolymers to the surface is too slow[58] to make this method practical. Alternatively, we have shown that thin block copolymer coatings of surface-active poly(styrene-*b*-dimethylsiloxane) block copolymers form spontaneously on polystyrene substrates when deposited from supercritical carbon dioxide.[59] This method also works well for the P(S-*b*-tBA) diblock copolymers used herein as will be reported shortly.[60] For the current study we have chosen to fabricate the surface block copolymer films by spin coating because this technique allows for excellent control of the block copolymer film thickness simply by changing the rotation speed and concentration of the solution used for spin coating.[61,62]

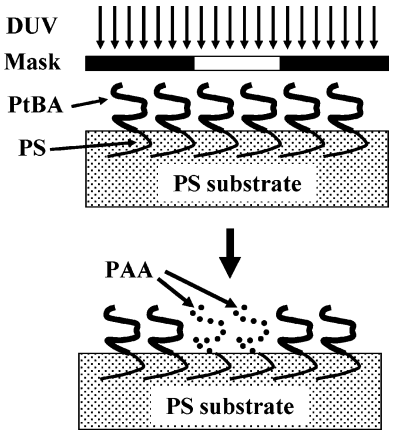

Figure 1. Strategy for surface photochemical patterning of P(S-*b*-tBA)-modified PS substrates. Exposure to DUV through a mask converts surface PtBA chains to PAA in illuminated regions.

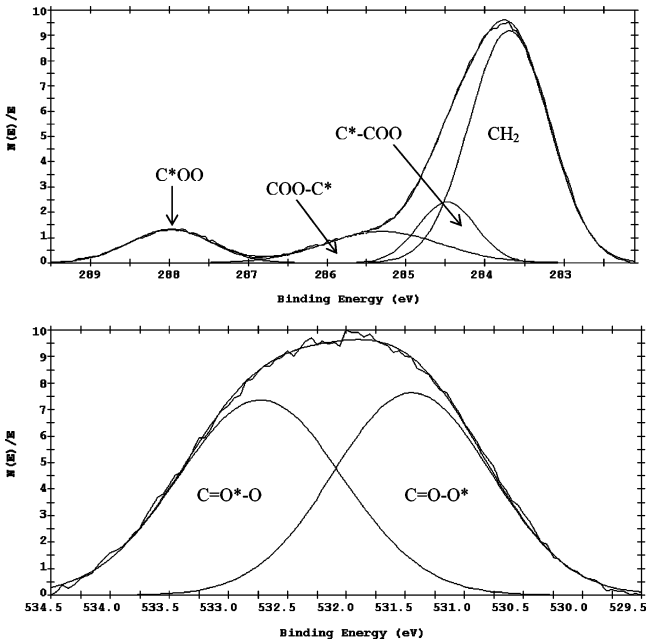

Figure 2. XPS high-resolution C 1s and O 1s spectra of P(S-*b*-tBA)-modified PS substrates showing the contributions of each carbon type. Note that the C 1s binding energy axis (BE) has not been internally referenced to the known binding energy of unshifted carbon at 284.6 eV.

Spin-coated films of block copolymer are expected to self-organize into a surface bilayer structure depicted schematically in Figure 1, presenting a surface layer of low surface tension poly(acrylate). Angle-dependent X-ray photoelectron spectroscopy measurements[63] are employed to confirm the formation of the bilayer structure. The ADXPS technique probes an integral depth of approximately $3\lambda \sin\theta$, where λ is the photoelectron mean free path and θ is the photoelectron takeoff angle, the latter defined as the angle between the photoelectron detector and a vector parallel to the sample surface.

A typical high-resolution carbon (i.e., C 1s) XPS spectrum of a P(S-*b*-tBA) block copolymer modified PS substrate is shown in the top half of Figure 2. Different chemical shifts in the BEs are observed due to carbon atoms existing in different chemical environments. The peak centered at 288.8 eV arises from the carbonyl carbon (C*OO−) in PtBA; the peak near 286.3 eV is ascribed to

(56) Schmitt, R. L.; Gardella, J. A., Jr.; Magill, J. H.; Salvati, L., Jr. *Macromolecules* **1985**, *18*, 2675.
(57) Hu, W. Koberstein, J. T.; Lingelser, J. P.; Gallot, Y. *Macromolecules* **1995**, *28*, 5209.
(58) Cho, D.; Hu, W.; Koberstein, J. T.; Lingelser, J. P.; Gallot, Y. *Macromolecules* **2000**, *33*, 5245.
(59) Cho, D.; Kim, Y.; Erkey, C.; Koberstein, J. T. *Macromolecules* **2005**, *38*, 1829.
(60) Wang, P.; Koberstein, J. T. Manuscript in preparation.
(61) Hall, D. B.; Underhill, P.; Torkelson, J. M. *Polym. Eng. Sci.* **1998**, *38*, 2039.
(62) Schubert, D. W. Dunkel, T. *Mater. Res. Innovations* **2003**, *7*, 314.
(63) Fadley, C. S. *Prog. Solid State Chem*. **1976**, *11*, 265.

Table 1. ADXPS Derived Elemental Compositions and Surface Composition for a Poly(S-*b*-tBA)-Modified Polystyrene Substrate Calculated for Various Photoelectron Takeoff Angles[a]

takeoff angle, deg	C	O	C*OO	COO−C*	C*−COO	C*(av)	ϕ_{PtBA}
10	76.85	23.15	12.93	12.07	16.38	13.79	0.970
15	78.09	21.91	11.35	12.28	15.9	13.18	0.931
30	79.79	20.21	11.62	12.38	10.37	11.46	0.822
45	81.50	18.50	9.62	11.03	12.54	11.06	0.797
75	81.87	18.13	7.92	8.96	10.89	9.26	0.678

[a] Elemental compositions are listed as percentages. The binding energy shifted bands are C*OO (BE = 288.8 eV), COO−C* (BE = 286.4 eV), and C*-COO (BE = 285.4 eV). C*(av) represents the average value of the three BE-shifted carbon elemental compositions. The error in elemental composition is approximately ±5%.

the ester carbon (COO−C*) in PtBA; and the peak centered at 285.4 eV is associated with the carbon adjacent to the carbonyl group (C*−COO) in PtBA. The unshifted C 1s peak at 284.6 eV is associated with both backbone carbons in PtBA and all of the carbons in PS. A typical oxygen (O 1s) spectrum is shown in the bottom half of Figure 2. The spectrum is split into two contributions of equal magnitude. The shifted O 1s peak at 533.8 eV is assigned to the carbonyl oxygen (C=O*−O) in the ester group of PtBA, while the unshifted oxygen at 531.5 eV is the ester oxygen (C=O−O*) in PtBA. Their contributions to the XPS spectrum are equal in magnitude as expected from the molecular structure.

The average atomic percentages of each type of carbon and oxygen (O 1s) atoms were measured as a function of the photoelectron takeoff angle, and the results are listed in Table 1. Shallower depths are probed at lower takeoff angles. The data at the lowest takeoff angle, reflecting the composition of the outermost surface region (i.e., an integral depth of approximately 1.8 nm), indicates that this region is essentially pure PtBA. On the basis of the molecular structure of PtBA, the intensities of the three shifted carbon peaks are expected to be in the ratio of 1:1:1, the intensity ratio of the oxygen 1s signal to the sum of the signals from the three shifted carbon atoms should be 2:3, and the ratio of total oxygen to total carbon should be 2:7. The experimental values for these ratios are all similar to the theoretical ones indicating that a layer of pure PtBA exists at the surface of the modified substrate.

The surface molar composition of PtBA, ϕ_{PtBA}, may be directly calculated by taking the ratio of the average intensity of the three BE-shifted C 1s signals, $I(\theta$, C 1s-shifted) equivalent to c*(av) in Table 1, to the total C 1s signal

$$\frac{I(\theta, \text{C 1s-shifted})}{I(\theta, \text{C 1s-total})} = \frac{\phi_{PtBA}}{7\phi_{PtBA} + 8(1 - \phi_{PtBA})} \quad (1)$$

This relationship is simply a mass balance where the first term in the denominator represents the contribution of the seven carbon atoms from a PtBA repeat unit and the second term represents the contribution for the eight carbon atoms in the polystyrene repeat unit. The surface composition determined by (1) represents an average over the sampling depth, and the results are reported in Table 1 as a function of the photoelectron takeoff angle. The surface composition approaches unity as the sampling depth decreases, confirming the existence of a pure surface layer of PtBA covering the block copolymer modified substrate, consistent with the bilayer model depicted in Figure 1.

ADXPS was then applied to quantitatively determine the thickness of the PtBA surface layer for the bilayer model. Because ADXPS is an integral technique, the signal from a particular atomic species is given by[63]

$$I_i(\theta) = k \int_0^\infty n_i(x) \exp\left(\frac{-x}{\lambda \sin \theta}\right) dx \quad (2)$$

where k is an instrumental factor. For the bilayer model, the ratio of C 1s signals from the average of the three binding-energy-shifted carbon atoms (i.e., c*(av) in Table 1) to the total carbon signal can be therefore be expressed as

$$\frac{I(\theta, \text{C 1s-shifted})}{I(\theta, \text{C 1s-total})} = \frac{\frac{N_{tBA}}{7}\int_0^d \exp\left(\frac{-x}{\lambda \sin \theta}\right) dx}{N_{tBA}\int_0^d \exp\left(\frac{-x}{\lambda \sin \theta}\right) dx + N_S \int_d^\infty \exp\left(\frac{-x}{\lambda \sin \theta}\right) dx} \quad (3)$$

Here d is the thickness of the PtBA surface layer, N_{tBA} is the total carbon atomic density in the PtBA layer, and N_S is the total carbon atomic density in the underlying PS layer. Rearrangement of (3) yields a relationship that can be graphically analyzed to calculate the thickness, d, of the PtBA surface layer

$$R(\theta) = \ln\left(\frac{1 - 7\frac{I(\theta, \text{C 1s-shifted})}{I(\theta, \text{C 1s-total})}}{1 + 7\frac{I(\theta, \text{C 1s-shifted})}{I(\theta, \text{C 1s-total})}\left(\frac{N_S}{N_{tBA}} - 1\right)}\right) = \frac{-d}{\lambda \sin \theta} \quad (4)$$

A plot of $R(\theta)$ against 1/sin θ should therefore be linear with a slope equal to $-d/\lambda$. An example of a typical plot of this nature is shown in Figure 3. The plot is linear, consistent with the expectations for the bilayer model. The absolute value of the thickness measured in this way is dependent on the value adopted for the photoelectron mean free path. If a mean free path of 3.1 nm[64] is assumed, the regression of (4) to the data (solid line in Figure 3) yields 1.5 nm for the thickness of the PtBA layer. Because the calculated thickness depends on the value of the mean free path assumed, the two values should always be reported together to be meaningful.

The thickness of the PtBA surface layer can be controlled by adjusting either the rotational velocity of the spin coater or the concentration of the polymer solution employed for spin coating.[61,62] The ability to control the thickness of the PtBA surface layer is illustrated in Figure 4, where the ADXPS-estimated PtBA layer thickness is shown as a function of the copolymer concentration in the spin coating solution. The dependence is linear as predicted by theory and illustrates that it is straightforward to control the

(64) Lukas, J.; Jezek. B. *Collect. Czech. Chem. Commun.* **1983**, *48*, 2909.

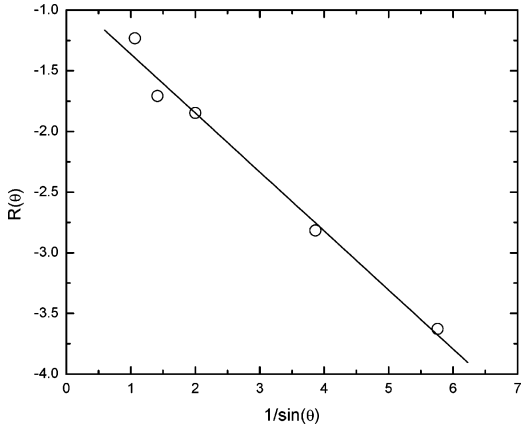

Figure 3. ADXPS estimation of the PtBA surface layer thickness according to the substrate-overlayer model (eq 4).[63]

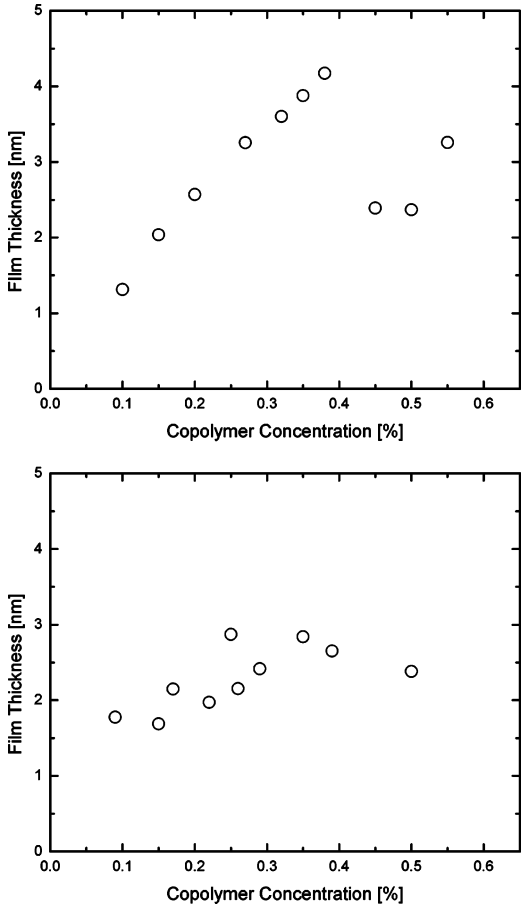

Figure 4. Thickness of the PtBA surface layer as a function of copolymer concentration in the initial spin coating solution: after annealing (a, top); directly after spin coating (b, bottom).

thickness of the photoactive polymer layer (i.e., PtBA) delivered to the surface. The data in the figure also demonstrate that annealing the spin coated films is beneficial to achieve the best organization of the surface-bound copolymers since the substrate is a glassy polymer. The annealing temperature was chosen at 110 °C, above the glass transition temperatures of both the PS (T_g = 100 °C) and PtBA (T_g = 45 °C) block copolymer sequences.

The PtBA surface layer thickness for annealed samples drops and seems to remain constant around 2.2 nm when the concentration exceeds 0.4 wt %. Previous experience suggests that this phenomenon is related to surface saturation and that full monolayer coverage of the block copolymer is achieved at a polymer concentration of about 0.4%. Higher concentrations result in partial multilayer formation in which case the ADXPS model becomes inappropriate. The radius of gyration of the PtBA block is estimated to be 11 nm,[65] much larger than the thickness of the PtBA surface layer. The PtBA sequences in the surface layer therefore do not form an extended brush structure.

The second step in our surface modification procedure is to expose the surface-bound block copolymer to UV radiation in order to deprotect the ester groups on the polyacrylate to produce functional, surface-bound poly(acrylic acid) as is illustrated in Figure 5. Exposure to UV radiation causes the PAG to release protons that hydrolyze the ester linkages to produce a carboxylic acid. Water contact angle analysis readily demonstrates the change from the hydrophobic PtBA surface with a contact angle of 90° to the hydrophilic PAA surface with a contact angle of 35°. The success of UV-induced deprotection is confirmed by the XPS C 1s spectrum in Figure 6. The tertiary carbon of the ester group (i.e., COO−C*), with binding energy of 286.6 eV, is absent from the spectrum indicating essentially complete loss of the *tert*-butyl protecting group

The third section of results demonstrates how the photochemical surface modification strategy can be used to pattern chemical functionality at surfaces and how these chemical patterns can be employed to template the spatial arrangement of biomolecules on a polymeric substrate. Figure 7 shows an optical micrograph of a block copolymer modified surface exposed to UV radiation through a contact mask in the presence of a PAG, after subsequent removal of the PAG-containing surface film. An image of the contact mask is clearly evident even in optical microscopy, perhaps due to the thickness change induced by loss of the *tert*-butyl groups. While the pattern resolution was not directly measured in this work, it should be similar to that of DUV photoresist technology using photoacid generators and fall in the micrometer to submicrometer range.

The optical image, however, does not prove that there is any difference in chemical structure at the surface. For this purpose, surfaces were decorated by physisorption of fluorescent dyes and characterized by fluorescence confocal microscopy. Derivatized dyes were selected so as to selectively adsorb to either hydrophobic *tert*-butyl ester functional regions or hydrophilic carboxylic acid functional regions on the surface. Specifically, the hydrophobic Bodipy-ester dye was used to image hydrophobic regions, while the hydrophilic Bodipy-NH2 dye was chosen to image hydrophilic carboxylic acid functional regions. Figure 8 (upper left) shows the image of the surface pattern obtained by preferential adsorption of the hydrophobic Bodipy-ester dye onto PtBA regions that were protected by the photomask from UV exposure. The pattern is therefore identical in shape to the pattern of the mask. Figure 8 (bottom) shows the fluorescent intensity traced along the solid dark line in the image at top left. The spatial periodicity of the fluorescence intensity is 100 μm, identical to that of the photomask. Figure 8 (top right) contains the image of the surface decorated by adsorption of hydrophilic Bodipy-NH_2. In this case, the dye associates with the PAA regions produced by UV exposure, most likely due to electrostatic attraction between the NH_3^+/COO^- pair which is formed after one proton from the surface −COOH group transfers to the terminal NH_2 group in the Bodipy-NH_2 dye in the presence of water. The patterns generated in this study were found to be stable when exposed to aqueous solutions used to decorate the surfaces with dyes and biomolecules.

(65) *Polymer Handbook*, 3rd ed.; Brandrup, J., Immergut, E. H., Eds.; Wiley: New York, 1989.

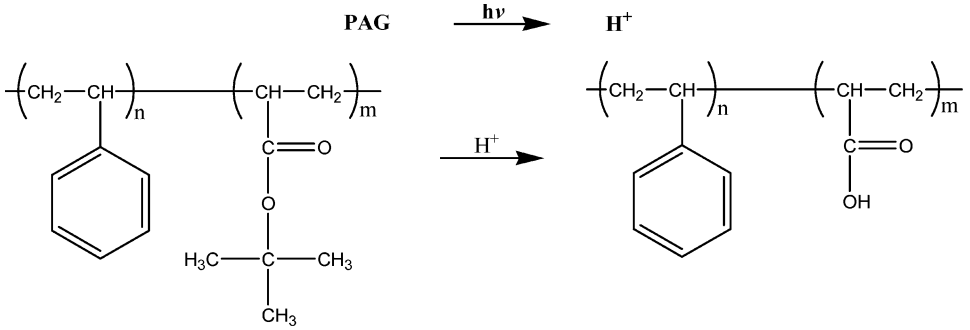

Figure 5. Schematic representation of the acid-catalyzed deprotection of P(S-*b*-tBA) to form P(S-*b*-AA).

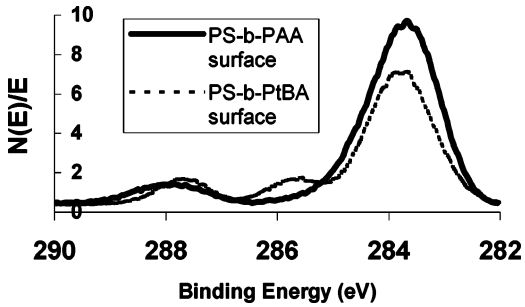

Figure 6. High-resolution XPS C 1s spectra before (solid line) and after (dashed line) UV exposure to deprotect the *tert*-butyl groups of PtBA on P(S-*b*-tBA) modified PS substrates.

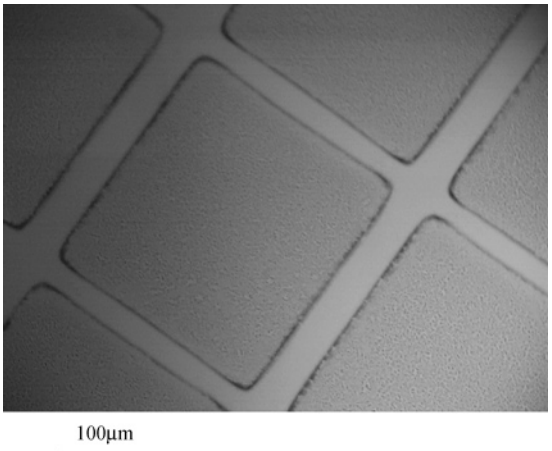

Figure 7. Optical photomicrograph of a patterned P(S-*b*-tBA)-modified PS substrate. The bar at lower left indicates 100 μm.

The chemically patterned substrates are also effective in templating the adsorption of proteins. Figure 9a illustrates that the plasma protein bovine serum albumin (BSA, MW ~ 69 kDa) selectively adsorbs onto PtBA regions of the patterned surfaces. Each BSA molecule typically has one to three hydrophobic tails comprised of fatty acid segments that associate with unconverted hydrophobic PtBA regions protected from UV exposure by the photomask.

Biomolecules may also by patterned either by direct covalent bonding to the surface carboxylic acid groups or by molecular recognition to appropriate surface-bound receptors or ligands. To illustrate both principles simultaneously, we have patterned fluorescent streptavidin by molecular recognition to biotin that was bound covalently to surface carboxylic acid groups using a bioconjugation technique. Chilkoti et al.'s procedure[39] was followed to attach biotin to the surface which can subsequently bind with streptavidin as shown in Figure 10. The chemical state of the surface after each derivatization reaction was

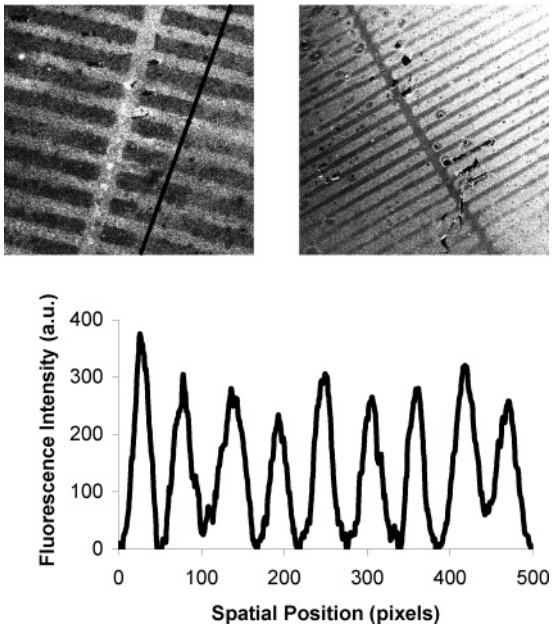

Figure 8. Fluorescence micrographs of patterned P(S-*b*-tBA)-modified PS substrates: contrast provided by preferential adsorption of Bodipy-ester (top left) and Bodipy-amine (top right). The figure at bottom shows the fluorescence intensity traced along the dark line delineated in the top left image.

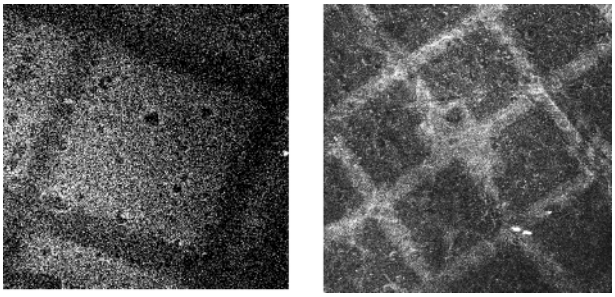

Figure 9. Fluorescence micrographs illustrating how BSA–FITC (left) and Streptavidin–Alexa488 (right) can be templated onto chemically micropatterned P(S-*b*-tBA)-modified PS substrates.

monitored by XPS as shown in Figure 11 and by the contact angle measurements summarized in Table 2. Activation of the COOH-functional surface sites of PAA by NHS/EDC mediation introduced a unique nitrogen 1s peak from NHS that is not present in the spectrum of PAA. The nitrogen peak persists in XPS spectra after coupling Biotin-NH_2 to the NHS/EDC activated PAA surface: however, the N 1s peak position shifts from 402.2 to 401.1 eV. The N 1s signal centered at 402.2 eV is consistent with the electron-withdrawing nature of nitrogen in NHS,

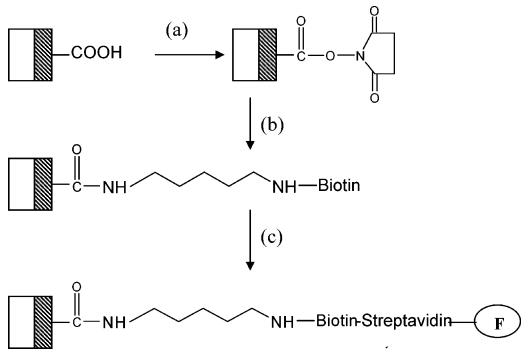

Figure 10. Schematic representation of streptavidin surface micropatterning: (a) NHS/EDC activation of surface carboxylic acid; (b) covalent coupling of biotin to the surface; (c) subsequent micropatterning of streptavidin by molecular recognition with immobilized biotin.

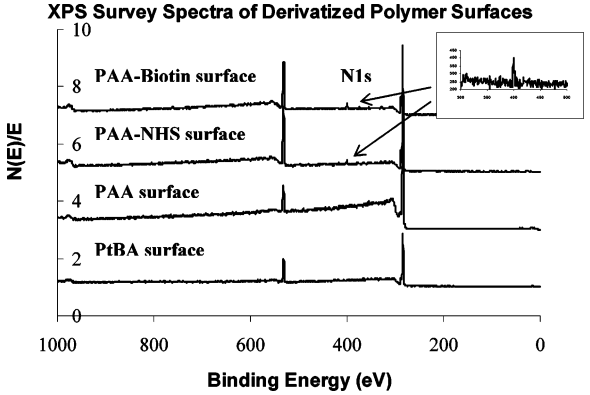

Figure 11. XPS survey spectra of derivatized polymer surfaces after each step in the surface immobilization of streptavidin. From bottom to top: the original PtBA surface, the PAA surface formed after deprotection of *tert*-butyl groups by UV exposure in the presence of a PAG, the PAA surface after activation of the carboxylic acid groups with NHS/EDC, the NHS activated surface after reaction with amine-terminated biotin.

Table 2. XPS Derived Elemental Compositions and Water Contact Angles for Derivatized Polymer Surfaces

material	% C	% O	% N	N 1s/C 1s	% yield	water contact angle, deg
PtBA	81.50	18.50	0	0	N/A	90 ± 3
PAA	74.04	25.96	0	0	N/A	35 ± 3
PAA−NHS	69.76	27.8	2.44	0.035	24.5	42 ± 3
PAA−Biotin	67.22	28.54	4.25	0.063	~100	5 7 ± 3

[a] Sessile drop water contact angles of several reference surfaces measured from spin coated thin film are: θs(PS) = 85°, θs(PAA) = 15°. The error in elemental composition is approximately ±5%.

and the lower BE (401.1 eV) N 1s is also consistent with the nature of the nitrogen present in biotin.

XPS-based elemental compositions and reaction yields, the latter calculated from N 1s/C 1s ratios, are also summarized in Table 2. The yield for each derivatization reaction was calculated by comparison of experimental and theoretical N 1s/C 1s ratios assuming that all reactive groups have been derivatized. For convenience the derivatized polymer surfaces are referred to as PtBA, PAA, PAA-NHS, and PAA−Biotin, respectively, at each stage. The N 1s/C 1s ratio was used to estimate the reaction yield instead of the N/O or O/C ratios because (1) N is only present after the activation and amidation reactions and (2) most surface contaminants are of high oxygen content and their presence therefore leads to an overestimate of the oxygen atomic composition.

The theoretical N 1s/C 1s ratio for the NHS/EDC activation step (see Figure 3) was calculated to be 0.143 assuming all surface −COOH groups are linked to NHS after activation. The experimental N 1s/C 1s ratio obtained from the XPS multiplex scan at a takeoff angle 45° was 0.035, so the reaction yield of this activation step was estimated to be 0.035/0.143 = 24.5%. A theoretical maximum N 1s/C 1s ratio of 0.222 is obtained similarly by assuming each PAA unit was linked with one biotin molecule after the amidation reaction. Taking into account that only ~24.5% of PAA groups are NHS/EDC activated and available for biotin linkage, the theoretical maximum N 1s/C 1s ratio is 0.222 × 0.245 = 0.054, close to the experimental N 1s/C 1s ratio of 0.063 after the amidation reaction. The excess nitrogen indicated by this result could arise from physisorption of Biotin-NH_2 to inactivated surface −COOH groups of PAA through electrostatic attraction or hydrogen bonding. Nevertheless, it suggests that the amidation reaction linking Biotin to PAA−NHS proceeds essentially to completion. The yields of both the activation and amidation steps are in good agreement with the literature.[39] Contact angle changes (Table 2) for the derivatized surfaces reflect the chemical modifications associated with each subsequent reaction step. Figure 9b presents a fluorescent micrograph of the end result: a copolymer-modified polymeric surface that first is first patterned with biotin by means of covalent attachment and then patterned again with fluorescently tagged streptavidin by molecular recognition with surface-bound biotin.

Conclusions

We report a novel and simple photolithographic approach that can be used to photochemically modify and micropattern the surfaces of most polymeric substrates. The method is based upon segregation of a photoactive block copolymer to the surface of a polymeric substrate, whereupon the copolymer self-assembles to form a bilayer structure presenting a surface layer of the photoactive polymer. In the example described, a p(S-*b*-tBA) copolymer self-assembles at the surface of a PS substrate to create a surface wetting layer of PtBA. The PtBA surface layer is converted to PAA by exposure to UV radiation in the presence of a photoacid generator. The success of surface modification is confirmed by XPS and water contact angle measurements. Surface chemical micropatterning is accomplished by simply exposing the copolymer-modified surfaces to UV radiation through a contact mask. Surface micropatterns are imaged by decoration with fluorescent dyes that selectively bind to particular regions of the patterned substrates by mechanisms that include electrostatic attraction and hydrophobic interaction. Two examples are presented to illustrate how the method can be used to template the deposition of biomolecules onto polymeric substrates: BSA−FITC is micropatterned on the surface of the modified polymeric substrate by virtue of hydrophobic interactions with PtBA regions and Streptavidin−Alexa488 is micropatterned via molecular recognition with biotin that is covalently bound to surface patterns of carboxylic acid groups.

Acknowledgment. This work was supported in part by U.S. Army Research Laboratory and the U.S. Army Research Office under Grant Number DAAD19-00-10104 and in part by the MRSEC Program of the National Science Foundation under Award Number DMR-0213574.

LA0477439